

# Narrowband Interference Suppression in CDMA Spread Spectrum Communications

Leslie A. Rusch, *Student Member, IEEE* and H. Vincent Poor, *Fellow, IEEE*

**Abstract**— Spread spectrum (SS) communications offers a promising solution to an overcrowded frequency spectrum amid growing demand for mobile and personal communications services. The proposed overlay of spread spectrum signals on existing narrowband users implies strong interference for the SS system. This paper discusses how system performance can be improved by preprocessing to suppress narrowband interference. Linear prediction filters have been proposed since the 1980s for suppression of narrowband interference. In 1991 Vijayan and Poor proposed nonlinear methods of suppressing the narrowband signal with significant increase in the SNR improvement. We derive an enhancement to this nonlinear prediction and achieve further improvement by applying the technique to interpolating filter structures. Finally, we extend results to the case of multiple spread spectrum users and demonstrate how nonlinear filtering can dramatically outperform linear filtering.

## I. INTRODUCTION

There is much concern in the communications industry with the increasingly overcrowded frequency spectrum, a condition aggravated by the growing demand for mobile radio and personal communications services. The use of spread spectrum techniques for these emerging multiuser environments has been proposed as a means of overlaying new mobile systems on existing band occupants, thereby relieving the demand for new allocations.

The proposed overlay of spread spectrum signals on existing narrowband users presents an opportunity for new nonlinear techniques in signal processing. Single user frequency bands can be modeled with some accuracy as having a Gaussian environment, however the presence of additional data signals causes decidedly non-Gaussian behavior. Optimal detectors and receivers for such channels are therefore no longer linear. For interference suppression this means the filtering environment is a non-Gaussian one. Nonlinear filtering is one possible technique that can be profitably used in such environments.

While SS has inherent noise suppression capability (it is this characteristic of spread spectrum that suggests the new applications), this paper discusses how system performance can be further enhanced by preprocessing to suppress narrowband interference. Techniques for filtering of the SS signals to suppress narrowband interference have been studied

since the 1980s. Fixed and adaptive linear prediction filters were first used to suppress significant portions of the interference. Interpolating linear filters were found to give even greater interference suppression [1,2,3,4,5].

In 1991 Vijayan and Poor proposed nonlinear methods of predicting the narrowband signal that led to significant increases in the SNR improvement due to filtering [6]. This nonlinear method was derived from a system model that takes into account the non-Gaussian distribution of the observation noise (from the point of view of predicting the interferer, the observation noise consists of AWGN plus the data signal). The nonlinear filter effectively introduces soft decision feedback into conventional filtering, essentially removing the data signal, and reducing the filter adaptation to one in Gaussian white noise. Results were extended to environments with impulsive noise in [7].

In this paper we derive an enhancement to the nonlinear prediction techniques of Vijayan and Poor as well as a new interpolating nonlinear filter structure. Furthermore, we extend results to the case of multiple spread spectrum users and discuss some issues that arise in the analysis of the nonlinearities.

The paper is organized as follows. We begin, in Section II, with the premise that by exploiting the predictability of a narrowband interferer we can increase the signal to noise ratio at the input of a spread spectrum receiver. To explore this problem analytically, a discrete time, state space model of the interference is used. The non-Gaussian measurement noise in this prediction requires a nonlinear filter for optimal (minimum mean square error) prediction. An *approximate conditional mean* nonlinear recursive filter is introduced. Results for simulations comparing linear and nonlinear filters for the case of known statistics are presented.

Adaptive filtering is examined in Section III for the more realistic case when the statistics of the narrowband process are unknown. A linear least mean squares predictor is modified to incorporate the approximate conditional mean nonlinearity. Results for simulations of linear and nonlinear adaptive filtering are given, including an enhancement of the original adaptive algorithm, proposed in [6].

Interpolating filters are considered next, in Section IV, and a new interpolated approximate conditional mean is derived. A block implementation of the adaptive nonlinear interpolating filter is developed. Simulation results are given comparing interpolating and predicting filters.

These filtering methods (both recursive and adaptive)

Paper approved by Gordon L. Stüber, the Editor for Spread Spectrum of the IEEE Communications Society. Manuscript received February 9, 1993; revised June 8, 1993. This research was supported by the National Science Foundation under Grants NCR 90-02767 and CDA-91-21709. This paper was presented in part at the Third International Symposium on Personal, Indoor and Mobile Radio Communications, Boston, Massachusetts, October 19-21, 1992.

The authors are with the Department of Electrical Engineering, Princeton University, Princeton, NJ 08544

IEEE Log Number 9401599.

are applied to systems with more than one spread spectrum user in Section V. The nonlinearity in the approximate conditional mean filter introduces an offset to the prediction. The offset is estimated and removed.

In Section VI we discuss some relevant issues regarding analysis of the performance of nonlinear over linear filtering and also the issue of convergence to a steady state solution. Finally, in Section VII, we summarize the results of this analysis and give several possible future directions for research.

## II. ACTIVE INTERFERENCE SUPPRESSION TECHNIQUES

Narrowband interference in a spread spectrum signal can be actively suppressed by exploiting the discrepancy in bandwidth of the two signals. The spread spectrum signal is essentially unpredictable, while the narrowband signal can be predicted with some accuracy. Consequently, any prediction of a received signal consisting of spread spectrum signals plus narrowband interference will be a prediction primarily of the interfering narrowband signal. Previous researchers have investigated linear filtering techniques for interference suppression in SS. If the interference is wide sense stationary and the statistics are known, the Levinson-Durbin algorithm can be used to recursively solve for the optimal filter coefficients. For unknown statistics, several techniques exist to determine the optimal tap weights adaptively. Among these the least mean squares (LMS) algorithm is used most frequently due to ease of analysis and implementation [1].

### A. System Model

In order to describe and analyze the narrowband interference suppression problem, we will assume that the received signal is passed through a filter matched to the chip waveform and chip-synchronously sampled once during each chip interval, per Figure 1. The equivalent discrete time received signal will have components due to the spread spectrum signal,  $s_k$ , the narrowband interference,  $i_k$ , and the ambient white noise,  $n_k$ . The observation at sample  $k$  is then given by

$$z_k = s_k + i_k + n_k. \quad (1)$$

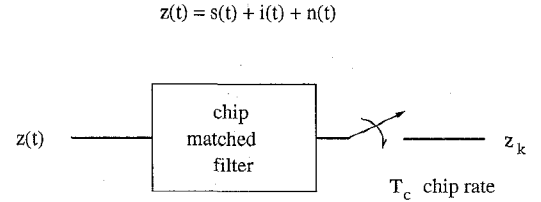
The ambient noise can be modeled as being white Gaussian with variance  $\sigma_n^2$ , the signal  $s_k$  as being  $\pm 1$  with equal probabilities, and the interference as having bandwidth much less than the spread bandwidth. The three signals can be assumed to be mutually independent.

Vijayan and Poor cast the interference suppression problem in state space form for use with the Kalman-Bucy filter [6]. We will adopt this model as well. The interference is modeled as an AR process, *i.e.*,

$$i_k = \sum_{j=1}^p \phi_j \cdot i_{k-j} + e_k \quad (2)$$

where  $e_k$  is a white Gaussian process with variance  $\sigma_e^2$ . The state space representation of our system is given by

$$\underline{x}_k = \Phi \underline{x}_{k-1} + \underline{w}_k \quad (3)$$



- $z_k$  received signal
- $s_k$  spread spectrum signal
- $i_k$  narrowband interference
- $n_k$  measurement noise (AWGN)

Fig. 1 System Model

$$z_k = H \underline{x}_k + \nu_k. \quad (4)$$

where  $\underline{x}_k = [i_k \ i_{k-1} \ \dots \ i_{k-p+1}]^T$ ,  $\underline{w}_k = [e_k \ 0 \ \dots \ 0]^T$ ,  $H = [1 \ 0 \ \dots \ 0]$ , and  $\Phi$  is the companion matrix of the vectors  $\phi_1, \dots, \phi_p$ . The observation noise in our system,  $\nu_k$ , is a sum of the white Gaussian measurement noise,  $n_k$ , and the spread spectrum signal,  $s_k$ . The variance of the combined observation noise is  $1 + \sigma_n^2$  (after normalizing to the energy of the spread spectrum signal, and assuming it is equiprobable  $\pm 1$ ).

The Kalman filter is the optimal *linear* predictor for the model of (3)-(4), and it is the *optimal* predictor when the observation noise is Gaussian (see, *e.g.*, Poor [8]). In our system, a Gaussian noise assumption clearly does not hold, as the observation noise density is the convolution of that of the spread spectrum signal with the Gaussian noise distribution. The smaller the measurement noise power in relation to the SS signal, the more pronounced is this difference. In order to exploit this non-Gaussian behavior, Vijayan and Poor proposed use of nonlinear filtering.

### B. ACM Filter

Recall that the minimum mean squared error (MMSE) estimator of the state  $\underline{x}_k$  at a fixed time  $k$  given the previous observations is  $E[\underline{x}_k | z_0^{k-1}]$ , where  $z_0^{k-1}$  represents all observations from time 0 to time  $k-1$ . Using the above model, if the observation noise were Gaussian, this would imply that the state and observations were jointly Gaussian. In this case, the conditional mean (and hence the MMSE estimator) would also have a Gaussian distribution. The Kalman-Bucy recursions are based on this model of Gaussian observation noise. For the system model used here the measurement noise is clearly not Gaussian, and the optimal filter (that is, the exact conditional mean) is nonlinear with exponentially increasing complexity. For the general state space filtering formulation with non-Gaussian measurement noise, Masreliez proposed an approximation to this optimal filter [9]. In particular, Masreliez proposed that some, but not all, of the Gaussian assumptions used in the derivation of the Kalman filter be retained in defining a nonlinear recursively updated filter. He abandoned the

requirement that the observation noise be Gaussian. However, he retained a Gaussian distribution for the conditional mean, although it is not a consequence of the probability densities of the system (as is the case for Gaussian observation noise); hence the name *approximate conditional mean* (ACM) that is applied to this filter.

Due to space considerations, we must refer the reader to [9] for a derivation of the ACM filter, and to [6] for its application to the system model used here. The nonlinear filter derived from the ACM has the following recursive updates. The time updates are:

$$\bar{\mathbf{x}}_{k+1} = \Phi \hat{\mathbf{x}}_k \quad (5)$$

$$M_{k+1} = \Phi P_k \Phi^T + Q_k \quad (6)$$

The measurement updates are given by:

$$\hat{\mathbf{x}}_k = \bar{\mathbf{x}}_k + M_k H^T g_k(z_k) \quad (7)$$

$$P_k = M_k - M_k H^T G_k(z_k) H M_k \quad (8)$$

The predicted estimate  $\bar{\mathbf{x}}_k$  is the mean of  $\mathbf{x}_k$  conditioned on previous observations,  $E[\mathbf{x}_k | z_0^{k-1}]$ , and  $M_k$  is its covariance. The vector  $\hat{\mathbf{x}}_k$  is the filtered estimate and its conditional covariance matrix is  $P_k$ .  $Q_k$  is the covariance matrix of the state input (the AR process). Note that the time updates are identical to those of the Kalman filter. The terms  $G_k$  and  $g_k$  denote nonlinearities arising from the (non-Gaussian) distribution of the observation noise and are given by the following

$$g_k(z_k) = \frac{1}{\sigma_v^2} \left[ \epsilon_k - \tanh \left( \frac{\epsilon_k}{\sigma_v^2} \right) \right] \quad (9)$$

$$G_k(z_k) = \frac{1}{\sigma_v^2} \left[ 1 - \frac{1}{\sigma_v^2} \operatorname{sech}^2 \left( \frac{\epsilon_k}{\sigma_v^2} \right) \right], \quad (10)$$

where we have defined  $\epsilon_k$  as the innovation (or residual) signal and  $\sigma_v^2$  as its variance; that is

$$\epsilon_k = z_k - H \hat{\mathbf{x}}_k \quad \sigma_v^2 = H M_k H^T + \sigma_n^2. \quad (11)$$

Note that, without the nonlinear terms  $\tanh$  and  $\operatorname{sech}$ , the Masreliez recursions reduce to the (linear) Kalman-Bucy recursions.

The ACM filter provides decision feedback in the  $\tanh$  term; that is, it corrects the measurement by a factor in the range  $[-1, 1]$  that estimates the spread spectrum signal. When the filter is performing well, the variance term in the denominator of the  $\tanh$  is low. This means the argument of the  $\tanh$  is larger, driving the  $\tanh$  into a region where it behaves like the  $\operatorname{sgn}(\cdot)$  function, and thus estimates the spread spectrum signal to be  $+1$  if the residual signal  $\epsilon_k$  is positive, and  $-1$  if the residual is negative. On the other hand, when the filter is not making good estimates, the variance is high and  $\tanh$  is in a linear region of operation. In this region, the filter hedges its bet on the accuracy of  $\operatorname{sgn}(\epsilon_k)$  as an estimate of the spread spectrum signal. Here the filter behaves essentially like the (linear) Kalman filter.

In the above we have referenced all the power variables ( $\sigma_n^2$  and  $\sigma_i^2$ ) to the spread spectrum power, which we take

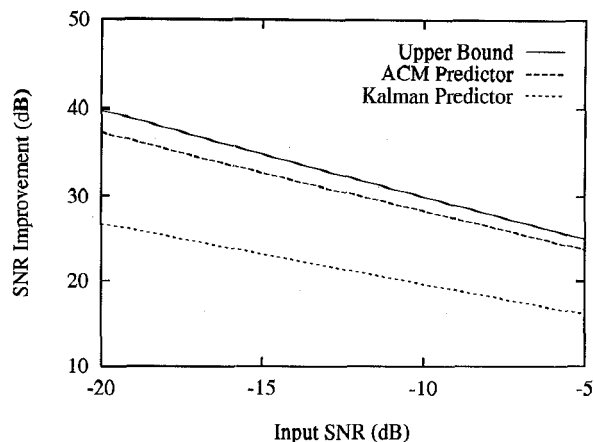


Fig. 2 Known Statistics

to be unity. When the power of the SS signal is not known at the receiver the  $\tanh$  term must be multiplied by an estimate of the amplitude. An adaptive algorithm for performing this estimate is described in [6].

### C. Simulations

In order to assess the performance gains afforded by the nonlinear techniques described above, simulations were run for a second order AR interferer with both poles at 0.99 (i.e.,  $\phi_1=1.98$  and  $\phi_2=-0.9801$ ). In this simulation, the noise power was held constant at  $\sigma_n^2 = 0.01$  while the total of noise plus interference power was varied from  $-20$  dB to  $5$  dB (all relative to a unity power SS signal). Our figure of merit in comparing filtering methods is the ratio of SNR at the output of filtering to the SNR at the input, which reduces to

$$\text{SNR improvement} = \frac{E(|z_k - s_k|^2)}{E(|\epsilon_k - s_k|^2)} \quad (12)$$

where  $\epsilon_k$  is defined as previously. The results for the Kalman predictor and ACM predictor are given in Figure 2. The filters were run for 1500 points. The results reflect the last 500 points, and the given values represent averages over 4000 independent simulations.

To stress the effectiveness against the narrowband interferer (vice the background noise), the solid line in Figure 2 gives an upper bound on the SNR improvement assuming that the narrowband interference is predicted with noiseless accuracy, that is, as  $\sigma_n \rightarrow 0$ . This is calculated by setting  $E(|\epsilon_k - s_k|^2)$  equal to the power of the AWGN driving the AR process, i.e., the unpredictable portion of the interference.

## III. ADAPTIVE FILTERING

### A. Linear Predictor

When the statistics for the AR process are not known, an adaptive algorithm must be used to find the optimal tap weights for the linear predictor. The LMS algorithm

is one of the simplest adaptive algorithms to analyze and implement. The linear predictor using an LMS filter of length  $L$  has the system diagram given in Figure 3. The residual of the prediction,  $\epsilon_k$ , is sent to the input of the SS receiver.

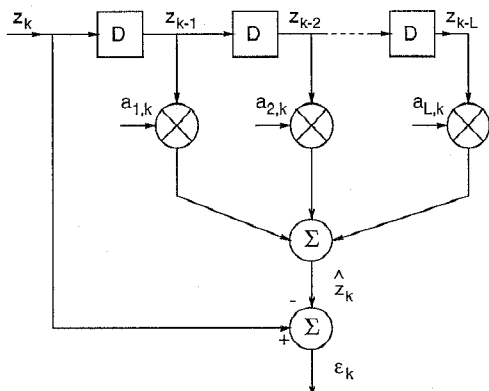


Fig. 3 Linear Predictor

For observation vector  $X_k = [z_{k-1} \ z_{k-2} \ \dots \ z_{k-L}]^T$  and vector of tap weights  $\Theta_k = [a_{1,k} \ a_{2,k} \ \dots \ a_{L,k}]^T$  at time  $k$ , the LMS filter generates the estimate  $\hat{z}_k = X_k^T \cdot \Theta_{k-1}$ , with tap weight updates

$$\Theta_k = \Theta_{k-1} + \mu_k (z_k - \hat{z}_k) \cdot X_k \quad (13)$$

A normalized step size  $\mu_k$  makes the step less dependent on the signal amplitude in  $X_k$  and also speeds convergence while guarding against instability. This step size is given by

$$\mu_k = \frac{\mu_0}{r_0 + r_k} \quad r_k = r_{k-1} + \mu_0 [|X_k|^2 - r_{k-1}]. \quad (14)$$

The estimate of the signal power  $r_k$  is an exponentially weighted estimate.  $\mu_0$  is chosen small enough to ensure convergence;  $r_0$  should be large enough so that the denominator never shrinks so small as to make the step size large enough for the adaptation to become unstable.

### B. Nonlinear Predictor

The nonlinearity appearing in the ACM filter has been introduced into the prediction structure in Figure 4. Assuming as before, that the prediction has a Gaussian distribution, then the distribution of the current observation conditioned on the previous observation is a sum of a Gaussian and a binary random variable. Denote by  $\sigma_k^2$  the variance of the innovation  $\epsilon_k$ ; then the appropriate nonlinearity is given by

$$\begin{aligned} \rho(\epsilon_k) &= z_k - \hat{z}_k - \tanh\left(\frac{z_k - \hat{z}_k}{\sigma_k^2}\right) \\ &= \epsilon_k - \tanh\left(\frac{\epsilon_k}{\sigma_k^2}\right). \end{aligned} \quad (15)$$

This transformation represents the residual less the soft decision on the SS signal. Let  $\bar{z}_k$  represent the observation

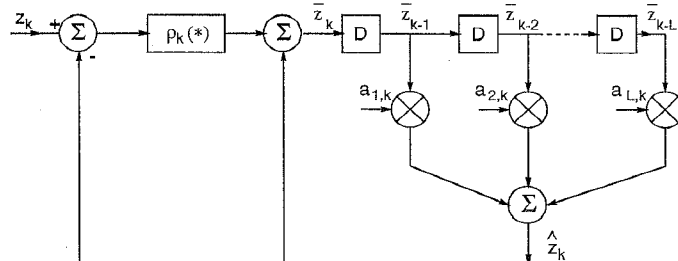


Fig. 4 Nonlinear Predictor

less the soft decision on the spread spectrum signal, that is,

$$\bar{z}_k = z_k - \tanh\left(\frac{\epsilon_k}{\sigma_k^2}\right) = \hat{z}_k + \rho(\epsilon_k). \quad (16)$$

Then Figure 4 represents the resulting adaptive nonlinear predictor. [6]

The filter weights  $\Theta_k$  are defined as for the linear predictor, as is the observation vector  $X_k$ . The nonlinear prediction is given by

$$\hat{z}_k = \theta_{k-1} \cdot [\bar{z}_{k-1} \ \bar{z}_{k-2} \ \dots \ \bar{z}_{k-L}]^T, \quad (17)$$

so that the estimate of the interference ( $\hat{z}_k$ ) is based on the observations *less* the soft decision on the signal. The tap weight update is unchanged, *i.e.*, (13). If the *tanh* function accurately tracks the SS signal, the filter essentially predicts the interference in white Gaussian noise and should only be limited by the unpredictable part of the AR process, the measurement noise and the excess error in the LMS algorithm.

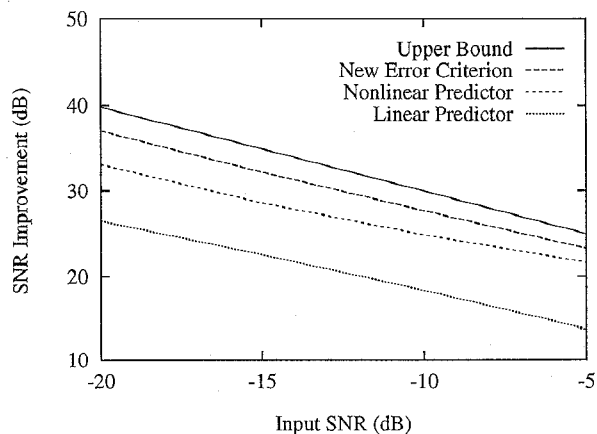


Fig. 5 Adaptive Filtering

### C. New Adaptation Algorithm

Previous simulations [6] showed that the adaptive nonlinear filter did not achieve the same performance as the ACM filter when foreknowledge of the interference statistics was used, whereas the linear filter did reach this prior

performance. This can be seen in comparing results in Figure 2 with Figure 5. By altering the tap weight update (13) to be based on the residual *less* the soft decision feedback, the adaptive filter was able to track the interference as well as the ACM filter did when the statistics are known. This new update equation is

$$\theta_k = \theta_{k-1} + \mu_k (\bar{z}_k - \hat{z}_k) [\bar{z}_{k-1} \bar{z}_{k-2} \dots \bar{z}_{k-L}]^T \quad (18)$$

Now the filter adaptation is indeed being done in Gaussian noise (when the decision feedback is accurate).

To assess this alternate adaptive algorithm, simulations were run on the same AR model for interference given in the previous section. Results given in Figure 5 are for averages over ten trials, with the SNR improvement calculated as a sample average of the last 500 points. The filter was run for 3000 samples. The new update strategy offers significant improvement over the earlier version of the adaptive ACM filter, which in turn performed much better than the linear filter. We observe that this adaptive algorithm achieves the same performance as do recursive filters that make use of the statistics of the interferer.

#### IV. INTERPOLATING FILTERS

Previous investigations into linear suppression filters led to the use of transversal, interpolating filters. In addition to the good phase characteristics of symmetric interpolating filters, these filters offered greater SNR improvement than predicting filters [2,4]. These results are extended to the Kalman and ACM filters in the following analysis. The goal of this line of research was to determine what gain (if any) could be obtained from an interpolating nonlinear filter, and how such a filter could be implemented. The first step is derivation of an interpolating ACM filter.

The following equations give the density of the current state conditioned on previous *and* following states. Although a slight abuse of notation, in the following derivation we let  $x_k = H\underline{x}_k$ , that is, the first component of the vector  $\underline{x}_k$ . The first relationship is a statement of Bayes formula.

$$p(x_k | z_0^{k-1}, z_{k+1}^N) = \frac{p(z_0^{k-1}, z_{k+1}^N | x_k) p(x_k)}{p(z_0^{k-1}, z_{k+1}^N)} \quad (19)$$

Using the independence of the  $z_0^{k-1}$  and  $z_{k+1}^N$  when conditioned on  $x_k$ , we can factor the first term in the numerator.

$$p(z_k | z_0^{k-1}, z_{k+1}^N) = \frac{p(z_0^{k-1} | x_k) p(z_{k+1}^N | x_k) p(x_k)}{p(z_0^{k-1}, z_{k+1}^N)} \quad (20)$$

Applying Bayes rule several times, we get the following.

$$= \frac{p(x_k, z_0^{k-1})}{p(x_k)} \frac{p(x_k, z_{k+1}^N)}{p(x_k)} \frac{p(x_k)}{p(z_0^{k-1}, z_{k+1}^N)} \quad (21)$$

$$= \frac{p(x_k, z_0^{k-1})}{p(z_0^{k-1})} \frac{p(x_k, z_{k+1}^N)}{p(z_{k+1}^N)} \frac{p(z_0^{k-1}) p(z_{k+1}^N)}{p(x_k) p(z_0^{k-1}, z_{k+1}^N)} \quad (22)$$

$$= \frac{p(x_k | z_0^{k-1}) p(x_k | z_{k+1}^N)}{p(x_k)} \cdot \frac{p(z_{k+1}^N)}{p(z_{k+1}^N | z_0^{k-1})} \quad (23)$$

The rightmost ratio of (23) is an integrating factor independent of the current state. If it is assumed (analogously to what is done in the Masreliez ACM filter) that the two densities in the numerator of the left term are Gaussian, then the interpolated estimate is also Gaussian. We use the notation  $\mathcal{N}(\mu, \Sigma)$  for a Gaussian density of mean  $\mu$  and covariance  $\Sigma$ . Therefore, if we assume the densities are as follows (where  $f$  indicates the forward prediction and  $b$  indicates the backward prediction)

$$p(x_k | z_0^{k-1}) = \mathcal{N}(\mu_f, \Sigma_f)$$

$$p(x_k | z_{k+1}^N) = \mathcal{N}(\mu_b, \Sigma_b)$$

$$p(x_k) = \mathcal{N}(\mu, \Sigma),$$

then the interpolated estimate is Gaussian with the following mean and covariance.

$$\begin{aligned} \text{mean} &= \mu_f^T \Sigma_f^{-1} [\Sigma_f^{-1} + \Sigma_b^{-1} - \Sigma^{-1}]^{-1} \\ &\quad + \mu_b^T \Sigma_b^{-1} [\Sigma_f^{-1} + \Sigma_b^{-1} - \Sigma^{-1}]^{-1} \quad (24) \end{aligned}$$

$$\text{covariance} = [\Sigma_f^{-1} + \Sigma_b^{-1} - \Sigma^{-1}]^{-1} \quad (25)$$

While the mean and covariance of the interpolated estimate at each sample  $k$  can be computed per the above equations, recall that the forward and backward means and covariance matrices are determined by nonlinear ACM-type filter recursions.

##### A. Block Interpolator for Known Statistics

The above equations can be used for both the linear Kalman filter and the Masreliez ACM filter to generate interpolated predictions from the forward and backward predicted estimates, ( $\mu_f$  and  $\mu_b$  respectively). As in the ACM predicting filter, we have approximated the conditional densities as being Gaussian, although the observation noise is not Gaussian. The filters are run forward on a block of data, and then backward on the same data. The two results are combined to form the interpolated prediction per (24).

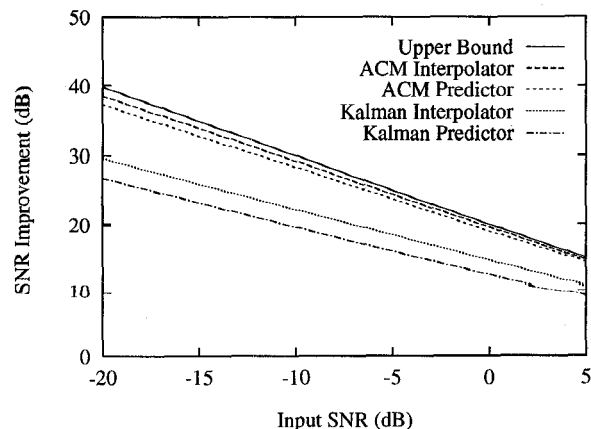


Fig. 6 Known Statistics - Interpolator

Simulations were run on the same AR model for interference given in the previous section. Figure 6 gives results for interpolated filtering over predictive filtering for the known statistics case. The filters were run forward and backward for all 1500 points in the block. Interpolator SNR gain was calculated over the middle 500 points (when both forward and backward predictors were in steady state). The results for the predictors reflect the last 500 points. All values represent averages over ten independent simulations. All filters used total tap lengths of 10.

### B. Adaptive Nonlinear Block Interpolator

As mentioned previously, linear interpolators were found to offer better SNR improvement than linear predictors [4], so the question arises as to whether an interpolating version of the nonlinear ACM adaptive filter gives similar improved performance over the ACM predictor. As seen in Figure 2, the margin for improvement in the ACM filter for the given interferer is not large, but if the additional complexity is not excessive, the added gain could be worthwhile.

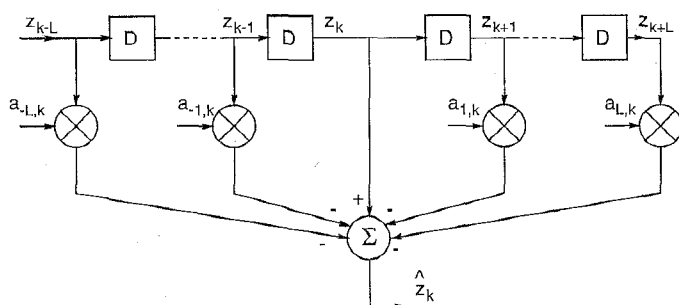


Fig. 7 Linear Interpolator

An FIR version of the linear interpolator is given in Figure 7. The equations for the interpolator are now given as follows.

$$X_k = [z_{k-L} \dots z_{k-1} z_{k+1} \dots z_{k+L}]^T \quad (26)$$

$$\theta_k = [a_{-L,k} \dots a_{-1,k} a_{1,k} \dots a_{L,k}]^T \quad (27)$$

where we set  $a_{-i,k} = a_{i,k}$  to ensure a linear-phase filter. The LMS algorithm is otherwise unchanged. When comparing the interpolating and predicting filters, the same number of tap weights is used. In the first case the taps are divided half before and half after the current sample. In the second case all the taps precede the current sample.

The ACM predictor is effective because it uses the interference prediction at time  $k$ ,  $\hat{z}_k$ , to generate a prediction of the observation less the SS signal,  $\bar{z}_k$ . This estimate  $\bar{z}_k$  is used in subsequent samples to generate new interference predictions. Initially the values of  $\bar{z}_1$  through  $\bar{z}_L$  are set equal to the observation at that sample. As time progresses each  $\bar{z}$  is generated by the previous prediction per

$$\bar{z}_k = z_k - \tanh\left(\frac{z_k - \hat{z}_k}{\sigma_k^2}\right) \quad (28)$$

where  $\sigma_k^2$  is a windowed average of the innovation variance.

The previous explains why the ACM filter cannot be cast directly in the interpolator structure seen in Figure 7. Estimates of  $\bar{z}$  are not available for samples that occur after the current sample. However, an approach similar to the one for the known statistics ACM interpolator can be used. In this approach the data is segmented in blocks and run through a forward filter of length  $L$  to give predictions  $\hat{z}_k^f$  and  $\bar{z}_k^f$ . The same data is run through a backward adaptive ACM filter with a separate tap weight vector, also of length  $L$ , to generate estimates  $\hat{z}_k^b$  and  $\bar{z}_k^b$ .

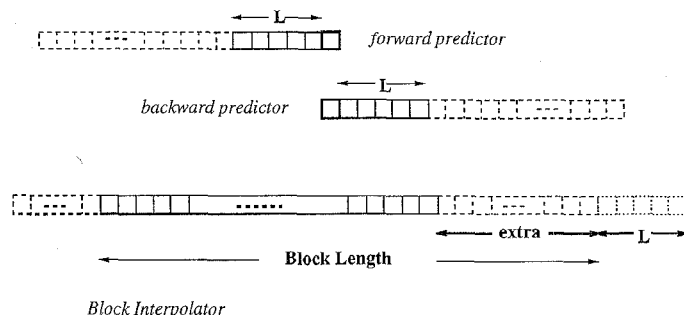


Fig. 8 Nonlinear Block Interpolator

After these calculations are made for the entire block, the data is combined to form an interpolated prediction per the following equations.

$$\hat{z}_k^i = \frac{1}{2}(\hat{z}_k^f + \hat{z}_k^b) \quad (29)$$

$$\bar{z}_k^i = z_k - \tanh\left(\frac{z_k - \hat{z}_k^i}{\sigma_k^2}\right) \quad (30)$$

Equation (24) would be the more accurate method to produce the estimate  $\hat{z}_k^i$ , however by the symmetry of the problem and for parameters used in our simulations, (24) is well approximated by (29). The next block of data follows the same procedure. However, when the next block is initialized the previous tap weights are used to start the forward predictor and the interpolated predictions  $\bar{z}^i$  are used to initialize the forward prediction  $\hat{z}^f$ .

This "head start" on the adaptation can only take place in the forward direction. We do not have any information on the *following* block of data to give us insight into the backward prediction. Therefore the backward prediction is less reliable than the forward prediction. To compensate for this effect, consecutive blocks are overlapped, with the overlap being used to allow the backward predictor some start up time to begin good predictions of the spread spectrum signal. This method of structuring the data is illustrated in Figure 8.

Results for the same simulation when the statistics are unknown are given in Figure 9. The adaptive interpolator had a block length of 250 samples, with 40% (100 samples) being overlapped. That is, for each block of 250 samples, 150 interpolated estimates were made. Results given in Figure 9 are for averages over ten trials, with the SNR

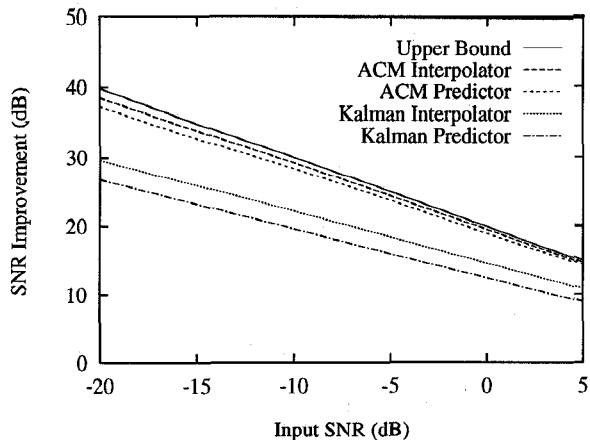


Fig. 9 Adaptive Filtering - Interpolator

improvement calculated as a sample average of the last 500 points. The filter was run for 3000 samples.

For the case of known statistics, the ACM predictor already performs well, and there is little margin for improvement via use of an interpolator. The adaptive filter shows greater margin for improvement, on which the interpolator capitalizes. However, in either case, the interpolator does offer improved phase characteristics and some performance gain at the cost of additional complexity (less than three times as many operations) and a delay (due to block length) in processing. The delay should be inconsequential in most spread spectrum applications and, depending on the hardware implementation of the ACM filter, the added complexity may also prove to be acceptable.

## V. MULTIPLE SS USERS

### A. Nonlinear Filter

The Masreliez filter equations can be applied to the case of more than one spread spectrum signal. To consider this situation, we use the same discrete time model of the system given in (3)-(4), *i.e.*,  $z_k = s_k + i_k + n_k$ . However, in this case, the spread spectrum signal  $s_k$  is the sum of  $N$  independent, equiprobable, binary, antipodal random variables and is binomially distributed. (We assume for tractability that the spread spectrum users are chip synchronous.) The measurement noise is the sum of AWGN and the (binomially distributed) spread spectrum signal, and its distribution is a binomially weighted Gaussian sum. The ACM filter for this distribution of the SS signal is derived, assuming that all users are received with the same (unit) power. By the Masreliez approximation, the state has a normal density when conditioned on the previous observations, *i.e.*,  $p(H\mathbf{x}_k) = \mathcal{N}(H\mathbf{x}_k, HM_k H^T)$  given  $z_0$  through  $z_{k-1}$ . Therefore the distribution of the current observation, conditioned on previous observations, is also a Gaussian mixture.

$$p(z_k = H\mathbf{x}_k + \nu_k) = 2^{-N} \sum_{j=1}^N \binom{N}{j}$$

$$\cdot \mathcal{N}(z_k - H\mathbf{x}_k - N + 2j, \sigma_n^2 + HM_k H^T) \quad (31)$$

Thus, defining  $\sigma_v^2 = \sigma_n^2 + HM_k H^T$ , we get the following equations for the Masreliez nonlinearities.

$$g(\epsilon_k) = \frac{\epsilon_k - N}{\sigma_v^2} + \frac{2}{\sigma_v^2} \frac{\sum_{l=1}^N l \binom{N}{l} e^{-(\epsilon_k - N + 2l)^2 / 2\sigma_v^2}}{\sum_{j=0}^N \binom{N}{j} e^{-(\epsilon_k - N + 2j)^2 / 2\sigma_v^2}} \quad (32)$$

$$G(\epsilon_k) = \frac{1}{\sigma_v^2} - \frac{1}{\sigma_v^4} f\left(\frac{\epsilon_k}{\sigma_v^2}\right) \quad (33)$$

where  $f(\cdot)$  is given by:

$$f\left(\frac{\epsilon_k}{\sigma_v^2}\right) = \frac{4}{\left[\sum_{j=0}^N \binom{N}{j} e^{-\frac{(\epsilon_k - N + 2j)^2}{2\sigma_v^2}}\right]^2} \sum_{l=1}^N \sum_{j=0}^N l(l-j) \cdot \binom{N}{l} \binom{N}{j} e^{-\frac{-(\epsilon_k - N + 2l)^2 + (\epsilon_k - N + 2j)^2}{2\sigma_v^2}} \quad (34)$$

Equation (32) is a smooth quantizer that returns an estimate of the SS signal. When the variance is high, this function is nearly linear between the extreme values of  $-N$  and  $N$ . When the variance is low, it acts like a step function taking values  $\{-N, -N+2, \dots, N-2, N\}$ . The nonlinearities in (32) and (33) reduce to the  $\tanh$  and  $\text{sech}^2$  functions when  $N$  is unity.

As the number of SS users increases, the total power of the SS signal grows. One would expect that as the power increases, the SS signal is even more easily distinguished from the noise and the Masreliez filter will track  $s_k$  with greater accuracy. Contrast this with the performance of the Kalman (linear) filter where the increased power of the SS signal causes the measurement noise to be even more highly non-Gaussian. Its performance will degrade as the number of users increases.

### B. Offset Problem and Compensation

Simulations were run for total input SNR of -20dB for the case of known statistics with the same AR model for the narrowband interference, letting the number of spread spectrum users vary. Results for runs of 10,000 samples are given in Table 1, where the increase in output SNR was measured in the steady state, *i.e.*, over the last 1000 samples. These results reflect averages over 4000 independent realizations.

The errors that are seen to occur in this first implementation of the Masreliez filter are due to improper referencing of the nonlinearity in (32). It can be shown that (given the filtered estimate  $\hat{\mathbf{x}}$  is initially set to the first  $p$  observations) the first soft decision feedback estimate of the SS signal is biased by a linear combination of the first  $p$  SS signal values. This leads to an initial error in the estimate of the interferer. The interfering signal is tracked well, but there is an offset in the predicted value  $H\mathbf{x}_k$  due to an incorrect first estimate of the spread spectrum signal. Once the offset is removed, the system should continue to make very good estimates of the predictable narrowband signal.

Number of users	SNR Improvement in dB			
	Kalman filtered	Masreliez filtered	Kalman predicted	Masreliez predicted
1	27.77	43.35	26.98	37.30
2	25.55	43.35	24.90	37.30
10	20.48	42.75	20.07	37.10
25	17.67	14.70	17.37	14.70
50	15.59	8.50	15.35	8.50

Tab. 1 Performance *without* offset being removed

Therefore simulations were redone estimating the offset at the start of operation and later subtracting it from our estimate of the interferer. After monitoring that the offset is indeed gone, we continue normal filter operation. Results are given in Figure 10. In this case the simulations were run for 1500 samples for 1 and 2 users, for 4000 samples for 10 users, for 5000 for 25 and for 7500 samples 50 users. All results are from averaging over the last 500 points of the run, and averaged over 4000 independent simulations.

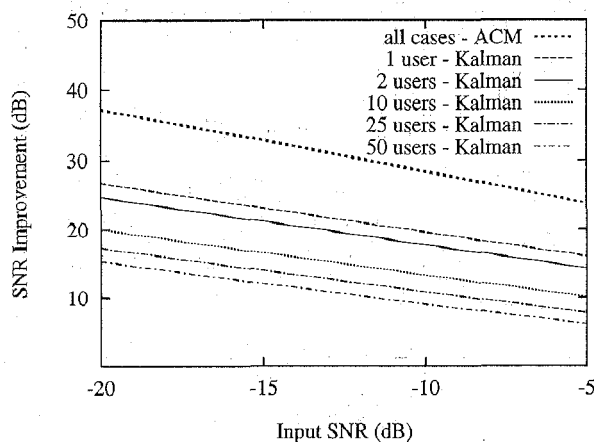


Fig. 10 Known Statistics - Multiple SS Users

### C. Adaptive Filtering

Adaptive filtering for the case of multiple SS users follows directly from the case of a single user. Again, there is an offset present due to the nonlinearity, which must be estimated and removed. Adaptation times were longer for multiple users, but performance tracked well with the results obtained for known statistics.

Simulations were run using the same AR parameters and the new adaptation algorithm given in section 3.3. After letting the adaptation run for some time, the offset was estimated and removed while adaptation continued.

Results are given in Figure 11 and reflect averages over the final 500 samples (in steady state) which were in turn averaged over 400 independent realizations. The filters

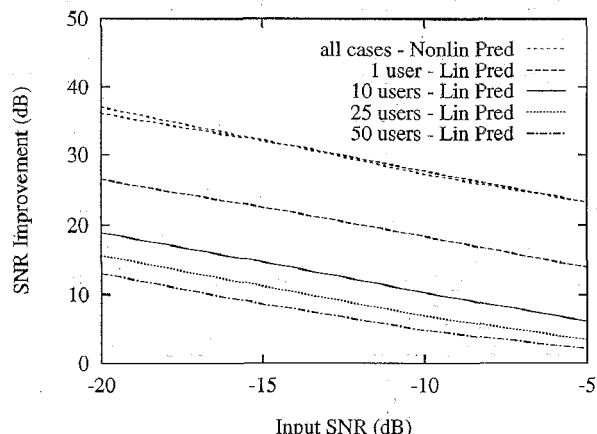


Fig. 11 Adaptive Filtering - Multiple SS Users

were allowed to run for 7,500 samples for 10 SS users, 10,000 samples for 25 users, and 12,500 for 50 users.

## VI. ANALYSIS OF NONLINEARITIES

Many fundamental results for the ACM filter remain open questions. In the case of Kalman filtering, it is well known that the covariance matrix will reach a steady state value when the magnitudes of the eigenvalues of the state transition matrix are less than unity. No similar criterion is known for the ACM filter. As pointed out by one of the reviewers, potential applications will depend upon the convergence speed of these nonlinear algorithms. Some preliminary discussion of convergence is included in this section, however the discovery of explicit convergence criteria and characterization of the rate of convergence are open research topics.

The simulations reported here are a dramatic demonstration that the ACM filter can outperform the Kalman filter. To what extent are they dependent on the parameters chosen for the simulation? Clearly the nonlinear method is effective because the measurement noise, AWGN and SS signal, is non-Gaussian. If the SS signal actually lies below the noise floor, then the Gaussian assumption is more reasonable, and the Kalman filter may actually outperform the nonlinear filter. Simulations show that for  $\sigma_n^2 > 1$  the Kalman filter and the nonlinear filter have virtually the same performance, and for values just below one the Kalman sometimes has a slight edge in performance. Note, however, that the ACM filter is never significantly outperformed by the Kalman filter since it reduces to the Kalman filter in the limit of vanishing signal power.

Similarly, the disparity of bandwidth between the existing users and the spread spectrum signal is essential for this filtering method and altering the AR model parameters (poles) will impact performance. Until criteria are known to guarantee (in a probabilistic sense) that the ACM performance will be better than that of the Kalman filter, we can only extend these simulation results by appealing to our intuition that the conditions of 1) low background (AWGN) noise relative to the spread spectrum signal and

2) the narrow bandwidth of the interferer relative to the spread spectrum signal are favorable conditions for this scheme to work.

We endeavor in the next sections to discuss how the data dependence of the ACM covariance update equation makes resolution of these questions a difficult analytical task. We draw on our experience with the simulations to make some observations about the behavior of the ACM filter.

#### A. ACM vs. Kalman Performance

We first address the issue of the relative performance of the ACM and Kalman filters, using the covariance of the predicted estimate as our metric. For Kalman filtering the covariance matrix is given by the following recursion.

$$\Sigma_{k|k-1} = \frac{\Phi \Sigma_{k|k-1} \Phi^T + Q + \Phi \Sigma_{k|k-1} H^T H \Sigma_{k|k-1} \Phi^T}{N + \sigma_n^2 + H \Sigma_{k|k-1} H^T} \quad (35)$$

As can be seen, this discrete time Riccati equation is independent of the data and the performance of the Kalman filter can be calculated offline from any observations. This is not the case for the ACM filter, whose covariance is governed by

$$M_{k|k-1} = \frac{\Phi M_{k|k-1} \Phi^T + Q + \Phi M_{k|k-1} H^T H M_{k|k-1} \Phi^T}{\sigma_n^2 + H M_{k|k-1} H^T} \left[ 1 - \frac{f\left(\frac{\epsilon_k}{\sigma_n^2 + H M_{k|k-1} H^T}\right)}{\sigma_n^2 + H M_{k|k-1} H^T} \right] \quad (36)$$

where  $f(\cdot)$  is given by (34). The argument of this nonlinear function  $f(\cdot)$  is dependent on the data, making this a *nonlinear stochastic difference equation*.

We have seen in the simulations that the ACM filter significantly outperforms the Kalman filter for the case of small ambient noise. One would then expect that as the ambient noise becomes vanishingly small, the covariance of the Kalman filter would exceed that of the Masreliez ACM filter. However, due to the data dependence of the Masreliez filter this property can only be stated in a probabilistic framework. To demonstrate this, we will assume that the Kalman and Masreliez filters are run on the same data, therefore with the recursions of equations (35) and (36) both started at  $\Sigma_{0|0}$ . We have then

$$M_{1|0} = \frac{\Phi \Sigma_{0|0} \Phi^T + Q + \Phi \Sigma_{0|0} H^T H \Sigma_{0|0} \Phi^T}{\sigma_n^2 + H \Sigma_{0|0} H^T} \left[ 1 - \frac{f\left(\frac{\epsilon_0}{\sigma_n^2 + H \Sigma_{0|0} H^T}\right)}{\sigma_n^2 + H \Sigma_{0|0} H^T} \right] \quad (37)$$

and,

$$\Sigma_{1|0} = \frac{\Phi \Sigma_{0|0} \Phi^T + Q + \Phi \Sigma_{0|0} H^T H \Sigma_{0|0} \Phi^T}{N + \sigma_n^2 + H \Sigma_{0|0} H^T} \quad (38)$$

Assuming that  $\sigma_n^2 \rightarrow 0$ , for the Masreliez covariance to be uniformly smaller we need to demonstrate that

$$\frac{H \Sigma_{0|0} H^T}{N + H \Sigma_{0|0} H^T} \geq 1 - \frac{f\left(\frac{\epsilon_0}{H \Sigma_{0|0} H^T}\right)}{H \Sigma_{0|0} H^T} \quad (39)$$

or,

$$f\left(\frac{\epsilon_0}{H \Sigma_{0|0} H^T}\right) \geq \frac{N \cdot H \Sigma_{0|0} H^T}{N + H \Sigma_{0|0} H^T} \quad (40)$$

For the case  $N = 1$ , this reduces to a requirement that

$$\sinh^2\left(\frac{\epsilon_0}{H \Sigma_{0|0} H^T}\right) \geq \frac{1}{H \Sigma_{0|0} H^T} \quad (41)$$

Given the initial value  $\Sigma_{0|0}$ , there is always an  $\epsilon_0$  sufficiently close to zero for which this inequality will not hold. The fact that the simulations always lead to a steady state value for the covariance is the result of the probability being extremely low that  $\frac{\epsilon_k}{\sigma_n^2}$  is in a sufficiently small neighborhood of zero. Since it is not true that the ACM filter's conditional covariance is less than that of the Kalman filter's at each sample, we must move to comparison of steady state values of the covariance.

#### B. Steady State Solution for ACM Covariance

As mentioned earlier, no criterion is known for the convergence of the ACM filter covariance to a steady state value. Indeed any such result would be a probabilistic convergence. During simulations we observed that the ACM covariance converged to a value equal to that of a Kalman filter with an input composed solely of the narrowband interference and AWGN. That is, in the steady state the ACM performed like a Kalman filter acting on observations from which the spread spectrum signal had been removed.

By comparing equation (35) with  $N = 0$  (Kalman filtering with the spread spectrum signal removed) and equation (36) (the ACM filter), we see that for these equations to reach the same value we should have

$$1 - \frac{1}{\sigma_n^2 + H M_{k|k-1} H^T} f\left(\frac{\epsilon_k}{\sigma_n^2 + H M_{k|k-1} H^T}\right) \approx 1 \quad (42)$$

Recall though that the simulations were run for benign SNR regions (*i.e.*,  $\sigma_n^2 \ll 1$ ). The approximation in equation (42) would not be valid for  $\sigma_n^2$  sufficiently close to one. So let us look at the relationship in equation (43) as  $\sigma_n^2 \rightarrow 0$ .

$$f\left(\frac{\epsilon_k}{H M_{k|k-1} H^T}\right) \ll H M_{k|k-1} H^T \quad (43)$$

For the case  $N = 1$ ,  $f(\cdot)$  is the *sech* function. The relationship in equation (43) for  $N = 1$  is plotted in Figure 12 for a continuum of variances ( $H M_{k|k-1} H^T$ ) and several values of the innovation ( $\epsilon_k$ ). If the ACM filter is accurately tracking the interferer, the innovation is just the spread spectrum signal and  $|\epsilon_k| = 1$ . As long as the error in the prediction is less than one half (which for  $N = 1$  means that  $|\epsilon_k| < .5$ ) our approximation is well justified. We see in the next section that this result is consistent with a model of ACM filter performance characterized by very low probability of mis-estimating the spread spectrum signal (as  $\sigma_n^2 \rightarrow 0$ ).

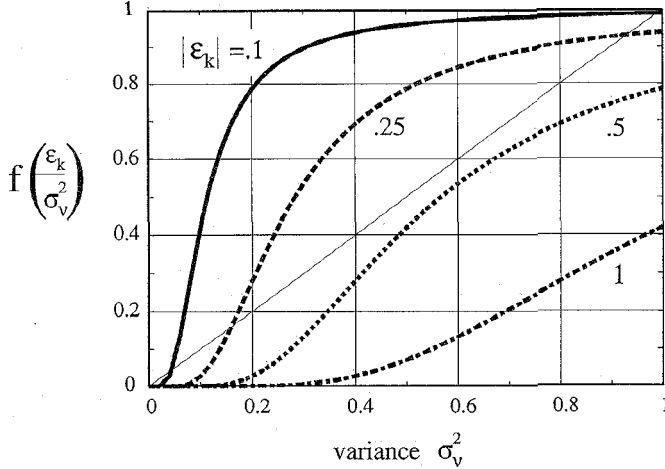


Fig. 12 Plot of  $f(\frac{\epsilon_k}{\sigma_v^2})$  versus  $\sigma_v^2$  for various values of  $|\epsilon_k|$

### C. Performance of ACM Filter in No Noise

In this section we investigate the performance of the filter in the limit as  $\sigma_n^2 \rightarrow 0$  and  $k \rightarrow \infty$  so that the filter is operating in steady state and in the absence of AWGN. The filtered estimate of the interferer is given by the following equation:

$$\hat{x}_k = \Phi \hat{x}_{k-1} + \frac{1}{\sigma_n^2 + H M_{k|k-1} H^T} \cdot M_{k|k-1} H^T (z_k - H \Phi \hat{x}_{k-1} - \hat{s}_k) \quad (44)$$

where  $\hat{s}_k$  is the estimate of the spread spectrum signal given by the nonlinearity

$$\hat{s}_k = f\left(\frac{z_k - H \Phi \hat{x}_{k-1}}{\sigma_n^2 + H M_{k|k-1} H^T}\right) \quad (45)$$

Letting  $\sigma_n^2 \rightarrow 0$ ,

$$\hat{x}_k = \Phi \hat{x}_{k-1} + \frac{1}{H M_{k|k-1} H^T} \cdot M_{k|k-1} H^T (z_k - H \Phi \hat{x}_{k-1} - \hat{s}_k) \quad (46)$$

$$\hat{s}_k = f\left(\frac{z_k - H \Phi \hat{x}_{k-1}}{H M_{k|k-1} H^T}\right) \quad (47)$$

Let us examine only the first component of  $\hat{x}_k$  which is the filtered estimate of the interferer, say  $\hat{i}_k$ .

$$\begin{aligned} \hat{i}_k &= H \hat{x}_k \\ &= H \Phi \hat{x}_{k-1} + \frac{H M_{k|k-1} H^T}{H M_{k|k-1} H^T} (z_k - H \Phi \hat{x}_{k-1} - \hat{s}_k) \\ &= z_k - \hat{s}_k \end{aligned} \quad (48)$$

So in the case of no AWGN, estimating the interference is equivalent to estimating the spread spectrum signal. So next we look at the estimate  $\hat{s}_k$ .

$$\hat{s}_k = f\left(\frac{z_k - H \Phi \hat{i}_{k-1}}{H M_{k|k-1} H^T}\right)$$

$$\begin{aligned} &= f\left(\frac{z_k - H \Phi (z_{k-1} - \hat{s}_{k-1})}{H M_{k|k-1} H^T}\right) \\ &= f\left(\frac{s_k + i_k - H \Phi (s_{k-1} + i_{k-1} - \hat{s}_{k-1})}{H M_{k|k-1} H^T}\right) \end{aligned} \quad (49)$$

Let  $\phi$  be the vector of coefficients for the AR process, *i.e.*,  $i_k = \phi \cdot [i_{k-1} \dots i_{k-p}]^T + e_k$ , then we can continue to substitute into (49) for  $\hat{s}_{k-1}$  for  $p$  times in order to eliminate  $i_k$ , until we get  $\hat{s}_k$  equals

$$f\left(\frac{e_k + s_k - \phi \cdot [(s_{k-1} - \hat{s}_{k-1}) \dots (s_{k-p} - \hat{s}_{k-p})]^T}{H M_{k|k-1} H^T}\right) \quad (50)$$

To continue the analysis we assume that the filter has been running long enough to arrive in the steady state and that the steady state value of  $H M_{k|k-1} H^T$  is small. In this case, the nonlinearity is operating in the regime of a step quantizer. For  $N = 1$  this means that  $f(\cdot)$  acts like the sigmoid function,  $\hat{s}_k$  equals

$$\text{sgn}(e_k + s_k - \phi \cdot [(s_{k-1} - \hat{s}_{k-1}) \dots (s_{k-p} - \hat{s}_{k-p})]^T) \quad (51)$$

Clearly if there are no errors in the previous  $p$  estimates,  $\hat{s}_k = \text{sgn}(e_k + s_k)$ . For the case of a very narrowband AR process (*e.g.*, double eigenvalues close to 1 for an order 2 process), the Gaussian noise driving the process will have power  $\sigma_i$  very small, even for large input interference. This means that the probability of error is characterized by a small value,  $Q(1/\sigma_i^2)$  (the complementary error function), in the steady state when no errors have occurred in the previous  $p$  samples, and a probability near one half after the next error does occur. Once the filter starts to make errors, the covariance will increase, driving the nonlinearity out of the sigmoidal function until steady state behavior can be reacquired.

## VII. CONCLUSION

In this treatment we have discussed the use of nonlinear techniques in systems with overlaid narrowband and spread spectrum signals. Simulations confirm that significant increases in the SNR at the SS receiver can be achieved when using nonlinear vice linear filtering, especially in the case of multiple spread spectrum users. Implementation of the nonlinear algorithm would require greater complexity than its linear counterpart which is typically encompassed in a single DSP chip. The functions  $\tanh$  and  $\text{sech}$  would either have to be calculated or stored in memory as a look-up table. As mentioned in the text, the interpolator would require on the order of three times as much calculation, and for multiple SS users a separate algorithm would be required to estimate the offset in the decision feedback.

The criterion for evaluating the performance in this paper was the SNR improvement. While a higher input SNR will lead to a lower BER, the quantitative improvement will not be as great. The processing gain of the SS signal will provide some interference suppression in its own right, for which both linear and nonlinear processing will benefit. This is a topic for further investigation. Also, because the proposed applications for commercial use of

spread spectrum will involve the overlaying of SS on existing narrowband users, the effectiveness of these techniques against several interferers should be investigated.

The study of the nonlinear stochastic difference equation describing the ACM covariance poses a research topic in its own right. Criteria to assure a probabilistic convergence of ACM covariance and a characterization of the convergence rate are needed, as well as convergence analysis of the adaptive nonlinear filter.

Finally, aside from the predictability of the narrowband process, the nature of the interferer itself may provide a key to better suppression techniques. Most existing band occupants will be digitally modulated waveforms of some variety. A more accurate model of the interferer may abandon the AR process in favor of a stochastic model of a digitally modulated signal. Multiuser detection could possibly be applied to suppress such narrowband users by modeling these signals as such.

#### REFERENCES

- [1] J. Ketchum and J. G. Proakis, "Adaptive algorithms for estimating and suppressing narrowband interference in pn spread spectrum systems," *IEEE Transactions on Communications*, vol. COM-30, pp. 913-924, May 1982.
- [2] L. Li and L. B. Milstein, "Rejection of pulsed cw interference in pn spread spectrum signals using complex adaptive filters," *IEEE Transactions on Communications*, vol. COM-31, pp. 10-20, January 1983.
- [3] L. Li and L. B. Milstein, "Rejection of narrowband interference in pn spread spectrum signals using transversal filters," *IEEE Transactions on Communications*, vol. COM-30, pp. 925-928, May 1982.
- [4] E. Masry, "Closed-form analytical results for the rejection of narrowband interference in pn spread spectrum systems - part ii: Linear interpolation filters," *IEEE Transactions on Communications*, vol. COM-33, pp. 10-19, January 1985.
- [5] E. Masry, "Closed-form analytical results for the rejection of narrowband interference in pn spread spectrum systems - part i: Linear prediction filters," *IEEE Transactions on Communications*, vol. COM-32, pp. 888-896, August 1984.
- [6] R. Vijayan and H. V. Poor, "Nonlinear techniques for interference suppression in spread spectrum systems," *IEEE Transactions on Communications*, vol. 38, pp. 1060-1065, July 1991.
- [7] L. Garth and H. V. Poor, "Narrowband interference suppression in impulsive channels," *IEEE Transactions on Aerospace and Electronic Systems*, vol. 28, pp. 15-34, January 1992.
- [8] H. V. Poor, *An Introduction to Signal Detection and Estimation*. Springer-Verlag, 1988.
- [9] C. J. Masreliez, "Approximate non-Gaussian filtering with linear state and observation relations," *IEEE Transactions on Automatic Control*, pp. 107-110, February 1975.

Leslie A. Rusch (S'81) was born in Chicago, Illinois, in 1958. She received her B.S.E.E. degree with honors from the California Institute of Technology in 1980, and the M.A. and Ph.D. degrees in Electrical Engineering from Princeton University in 1992 and 1994, respectively. After completing her bachelor's degree she worked as a project management engineer for the Department of the Army. Her current research interests include spread spectrum communications, personal wireless communications, and code division multiple access for radio and optical frequencies.

H. Vincent Poor (S'72 - M'77 - SM'82 - F'87) was born in Columbus, Georgia, in 1951. He graduated with highest honors from Auburn University in 1972, and received the Ph.D. degree in Electrical Engineering and Computer Science from Princeton University in 1977. In that year he joined the University of Illinois, where, from 1984, he was Professor of Electrical and Computer Engineering, and Research Professor in the Coordinated Science Laboratory. In 1990, he joined Princeton University where he is currently Professor of Electrical Engineering. He has also held visiting appointments at Imperial College (London) and at the University of Newcastle (Australia). Dr. Poor's current research interests are in the area of statistical signal processing, with applications in multiuser communications and acoustic signal processing. His publications in this area include the textbook *An Introduction to Signal Detection and Estimation*. He is a member of the Editorial Boards of several journals, including *Mathematics of Control, Signals and Systems*; the *International Journal of Imaging Systems and Technology*; and the *International Journal of Robust and Nonlinear Control*.

Dr. Poor is a Fellow of the American Association for the Advancement of Science; a Fellow of the Acoustical Society of America; and a member of the Institute of Mathematical Statistics. He has been involved in a number of IEEE activities, including as an Associate Editor of the *IEEE Transactions on Automatic Control* and of the *IEEE Transactions on Information Theory*; as Program Chair for the 25<sup>th</sup> IEEE Conference on Decision and Control (1986); as General Chair for the 1989 American Control Conference; as 1990 President of the IEEE Information Theory Society; and as a member of the IEEE Board of Directors from 1991-1992. He is currently serving on the Board of Governors of the IEEE Control Systems Society. In 1992, Dr. Poor received the Frederick Emmons Tenman Award from the American Society for Engineering Education.